Advanced Packed-Bed Ca-Cu Looping Process for the CO_2 Capture From Steel Mill Off-Gases

José Ramón Fernández[1]*, Vincenzo Spallina[2] and Juan Carlos Abanades[1]

[1] Spanish Research Council, Instituto Nacional de Ciencia y Tecnología del Carbono (INCAR-CSIC), Oviedo, Spain,
[2] Department of Chemical Engineering and Analytical Science, University of Manchester, Manchester, United Kingdom

A novel configuration of the Ca-Cu looping process based on dynamically operated packed-bed reactors is proposed to convert blast furnace gas (BFG) into H_2/N_2 and highly concentrated CO_2, accompanied by a large amount of high-temperature heat. Preliminary energy and mass balances of the process reveal that around 30% of the BFG can be upgraded via calcium assisted water gas shift (WGS) if only BFG is used as reducing gas in the reduction/calcination stage. A higher amount of H_2/N_2 can be produced by using other steel mill off gases, such as coke oven gas (COG) or basic oxygen furnace gas (BOFG), or natural gas in the regeneration of the CO_2 sorbent. This decarbonized fuel gas could be used for onsite power generation or to obtain sponge iron by a Direct Reduced Iron (DRI) process, increasing the overall capacity of the steel plant. Energy efficiencies higher than 75% have been calculated, reaching maximum values around 88% in case of using natural as fuel gas for the sorbent regeneration stage. Low values for the specific energy consumption of around 1.5 MJ_{LHV}/kg_{CO2} and CO_2 capture efficiencies higher than 95% support the further development of the proposed Ca-Cu looping process.

Keywords: CO_2 capture, hydrogen, steel mill, chemical looping combustion, calcium looping, energy efficiency

INTRODUCTION

Iron and steel production is a very energy-intensive industry (i.e., around 20 GJ are demanded for the production of 1 ton of steel) and accounts for around 7% of total CO_2 emissions (Cavaliere, 2019). Nowadays, more than 1700 million tons of crude steel are annually produced and the demand for steel will continue growing for the next decades until it approaches 2600 million t/year by 2050 (ArcelorMittal, 2019). The steel sector faces the need for dramatically reducing carbon emissions (i.e., 50% reduction by 2050 and reach net zero CO_2 emissions by 2100) to comply with the challenging climate change mitigation targets agreed after COP21, which are aimed at limiting the increase in global temperature to 1.5°C (IPCC, 2018).

About 70% of steel produced worldwide is obtained through the Blast Furnace-Basic Oxygen Furnace (BF-BOF) process, which generates around 1.8 tons of CO_2 per ton of crude steel (IEA Report, 2017). Another option is to produce steel from scrap via Electric Arc Furnace (EAF), where the solid iron is melted by electric power. This alternative allows a reduction of above 50% in the energy demand, but the process is limited by the availability of scrap and the quality requirements of the steel (IEAGHG, 2013; ZEP, 2015). Finally, the Direct Reduced Iron (DRI) can reduce the carbon footprint by 25% compared to conventional blast furnaces (IEA Report, 2019). In the

commercialized varieties of this technology (i.e., Midrex and Hylsa), natural gas is converted into a syngas that acts as reductant agent instead of coke. Iron ore is reduced to metal iron in the shaft furnace and subsequently fed into an electric arc furnace to produce steel (Ho et al., 2013; Bechara et al., 2018).

In this context, CO_2 Capture and Storage (CCS) must play a decisive role in decarbonizing the steel production far beyond the current levels achieved with existing technologies (IPCC, 2018). The post-combustion technologies that use aqueous solutions with amines can be applied in principle to remove the CO_2 from steel mill off-gases. However, the relatively high energy requirements for amine regeneration and the limited chemical stability showed in the long term have hampered so far the deployment of this technology in steel plants (Arasto et al., 2013; Tsupari et al., 2013). During the VALORCO project, the investigations were focused on the development of advanced amine-based sorbents that showed high CO_2 sorption capacity (four times higher than aqueous monoethanolamine, MEA) and negligible degradation after a large number of cycles (Dreillard et al., 2017). The demonstration of this technology in operational environment at pre-commercial scale (i.e., at Technological Readiness Level 7, TRL7) is the goal of the ongoing 3D Project (Lacroix et al., 2019). The first large-scale CO_2 capture plant installed in a steel industry operates since 2016 in Abu Dhabi with a capture capacity of 0.8 MtCO_2/year. This facility treats the shaft off-gas obtained in a DRI process and the separation of CO_2 is carried out by MDEA absorption (Sakaria, 2017).

During the Ultra-Low CO_2 Steelmaking project (ULCOS), Top Gas Recycling (TGR) was shown to be the most promising technology tested, which consists in injecting almost pure oxygen into the furnace instead of air. In these conditions, the high partial pressure of CO_2 in the product gas facilitates its subsequent separation downstream (typically by pressure swing adsorption). The gas free of CO_2, which mainly contains CO and H_2, is partially recirculated to the furnace to reduce the iron ore, thereby lowering significantly the need for coke in the process (IEAGHG, 2013; van der Stel et al., 2013; Jin et al., 2015). The COURSE50 programme has been focused on investigating the potential of H_2-rich gases, such as coke oven gas (COG), as reducing agents in the blast furnace instead of coke. In this line, novel chemical and physical adsorption methods have been developed to capture first the CO_2 from the blast furnace gas (BFG) and then use waste heat available in the steel plant for the regeneration of the sorbents (Tonomura, 2013; Nishioka et al., 2016).

Pre-combustion technologies to decarbonize the blast furnace gas (typically containing around 45%vol. of CO and CO_2) are attractive alternatives to significantly reduce the carbon footprint of the steelmaking process as the BFG contains more than 60% of the total CO_2 emitted by the plant. By means of a sorption enhanced water-gas-shift (SEWGS) process, the BFG is converted into a H_2-enriched gas (>30%vol H_2), whereas the CO_2 generated in the reactor is removed *in situ* due to the presence of a high-temperature sorbent (typically a hydrotalcite-based solid that is also water-gas-shift catalyst at temperatures between 300 and500°C) (Ji et al., 2018). The demonstration of this technology up to TRL6-7 has been carried out during the consecutive EU programmes CACHET, CAESAR, and STEPWISE (van Selow

et al., 2009; Boon et al., 2015; Gazzani et al., 2015). It has been observed that the main challenge for the scaling-up of the SEWGS process is the high cost for the sorbent regeneration and the low inherent CO_2 sorption capacity of the sorbent (best carrying capacities of promoted hydrotalcites have been measured at up to 8 wt.%).

CaO-based materials have been widely proposed as CO_2-sorbents in other pre-combustion applications (Harrison, 2008; Blamey et al., 2010; Martavaltzi et al., 2010), since they exhibit much larger CO_2 carrying capacities [ranging from 30 to 45%wt in newly developed CaO materials (Valverde, 2013; Erans et al., 2016)], very high theoretical energy recovery and they can be obtained from abundant and inexpensive natural sources. However, these processes have traditionally faced a major obstacle as CO_2 capture concept because they require high temperatures (around 900°C) to carry out the regeneration of the sorbent by $CaCO_3$ calcination in rich atmospheres of CO_2. Supplying a large thermal power input for regeneration [calcination requires a minimum of 3.9 MJ/kg of CO_2 evolved from calcination (Hills, 1967)] is a major engineering challenge, even if this energy can be effectively recovered during carbonation and heat recovery stages. One option is to combine the sorption enhanced reactions with chemical looping combustion, so that the large amount of energy needed for the calcination is supplied by the oxidation of Ni- (Antzara et al., 2015) or Fe-based oxygen carriers (Tian et al., 2016). Although these configurations avoid the need for large heat-transfer surfaces at very high temperature, they still require an air separation unit (ASU) to obtain a CO_2-rich gas during the decomposition $CaCO_3$ to CaO. In the Ca-Cu looping process, the exothermic reduction of CuO to Cu using a gaseous fuel (e.g., CH_4, CO, or H_2) supplies the necessary heat to carry out simultaneously the calcination of the carbonated sorbent producing exclusively CO_2 and H_2O without the presence of an ASU in the process (Fernández et al., 2012). A substantial progress has been made during the EU ASCENT project on dynamic reactor modeling (Martini et al., 2016, 2017; Fernández and Abanades, 2017a), development of Ca-Cu materials (Kazi et al., 2017), process integration (Riva et al., 2018; Martínez et al., 2019b), and experimental validation from small reactors to packed beds at TRL5 (Fernández and Abanades, 2017b; Grasa et al., 2017; Díez-Martín et al., 2018; Martínez et al., 2019a). Some recent works have proposed the use of the Ca-Cu based process to convert the BFG into valuable products, such H_2/N_2 and pure CO_2, using a combination of several interconnected fluidized beds operating in continuous mode (Fernández et al., 2017; Martínez et al., 2018). This configuration facilitates the heat management during the highly exothermic redox stages but it is limited in the operating pressure (only atmospheric) and requires a challenging solids segregation unit to separate the CaO- from the Cu-based materials once the sorbent has been regenerated.

We propose in this work a novel Ca-Cu looping configuration based on packed-bed reactors, that is able to operate at high pressure to transform blast furnace gas into a H_2-rich gas with higher LHV as well as a large amount of high-temperature heat. This decarbonized fuel gas can be used for onsite power generation or to obtain sponge iron by a
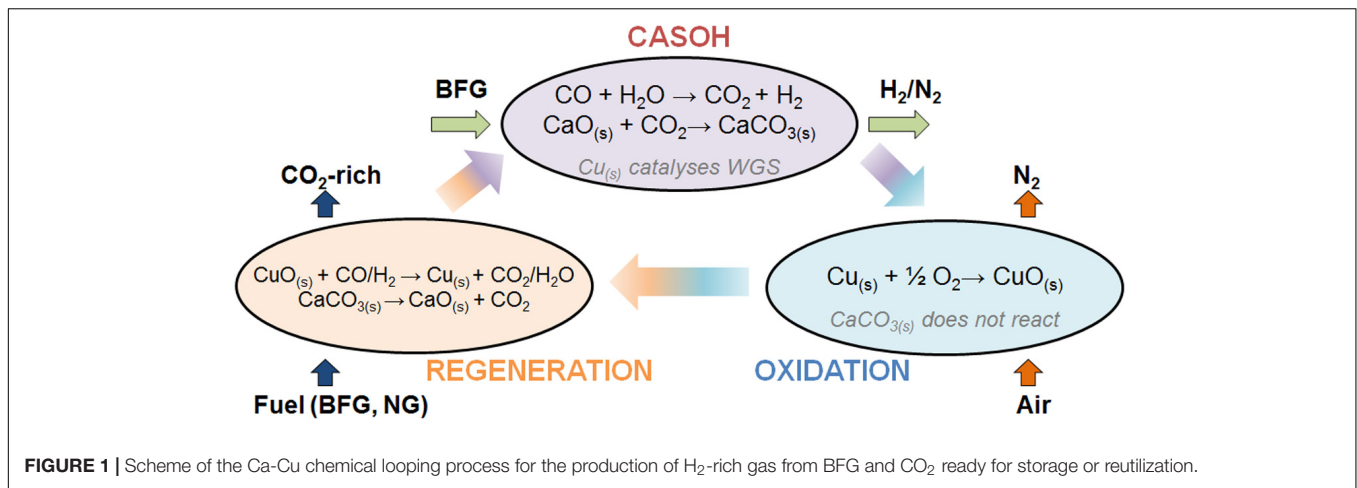
FIGURE 1 | Scheme of the Ca-Cu chemical looping process for the production of H_2-rich gas from BFG and CO_2 ready for storage or reutilization.

DRI process, increasing the overall capacity of the plant. The arrangement of several packed-bed reactor will perform in a sequence of three main reaction stages (i.e., BFG upgrading, Cu oxidation and CO_2 sorbent regeneration) following well established principles of dynamic operation as for other commercial PSA/TSA processes and regenerative heat-transfer processes (see simplified scheme in **Figure 1**). Four different configurations are considered here in terms of process operating conditions and fuel utilization. The performance obtained for the different Ca-Cu integrated plants will be compared in terms of primary energy consumption, product yields, CO_2 purity and potential CO_2 capture rate to demonstrate the theoretical viability of the process.

PROCESS DESCRIPTION

The Ca-Cu looping process allows great flexibility in the feedstock and a modular reactor configuration (i.e., in size and number of parallel units) is feasible. The main fuel off-gases of the steel mill (see characteristics in **Table 1**) can be decarbonized with this technology depending on the level of integration of the

Ca-Cu process, giving rise to a wide variety of products and uses (see **Figure 2**). The characteristics of the steel mill off-gases are listed in **Table 1** (Santos, 2013).

Apart from the BFG, which can be converted into a H_2/N_2 gas by means of an enhanced WGS process (explained above), the basic oxygen furnace gas (BOFG) (with around 60%vol. of CO) can also be valorized following the same procedure to produce separately a H_2-enriched gas (>75% purity), N_2 and pure CO_2. Moreover, the COG (with about 25 and 60%vol. of CH_4 and H_2, respectively) can be fed into a Ca-Cu chemical loop combined with sorption enhanced reforming (in a similar way to the process schemes reviewed in Martínez et al., 2019a) to obtain almost pure H_2 and N_2 useful for power generation o chemical synthesis (e.g., ammonia) (Martínez et al., 2017). Any possible combination of BFG, COG, and BOFG can be considered by tuning the Ca/Cu ratio in the reactors (Alarcón and Fernández, 2015) to obtain the desired products and the CO_2 capture rate that can range from 10 to 95%.

Among all the aforementioned possibilities, this work is focused on the valorization of the BFG, as it is by far the main off-gas emitted by a steelmaking plant. **Figure 3** shows the process scheme of the proposed Ca-Cu looping process for BFG, which is composed of several packed-bed reactors dynamically operated in parallel with alternating temperature and pressure to accommodate the conditions of every solids bed. The main stage of the process involves the production of a H_2/N_2 fuel gas (stream 4) through the water-gas-shift reaction of the CO contained in the BFG (around 23%vol.). In this stage, called Calcium Assisted Steel-mill Off-gas Hydrogen (CASOH) production, Cu-based particles act as WGS catalyst and the presence of CaO allows a substantial part of the CO_2 to be removed from the reacting atmosphere as soon as it is produced. The continuous elimination of CO_2 by the carbonation of the CaO-based sorbent shifts the WGS equilibrium toward a higher production of H_2, so that a very high conversion of the inlet CO is feasible at temperatures between 500 and 700°C. The resulting gas contains more than 30%vol of H_2 diluted with N_2 and very low amounts of CO and CO_2.

TABLE 1 | Composition of the steel mill off-gases used for the calculations (Santos, 2013).

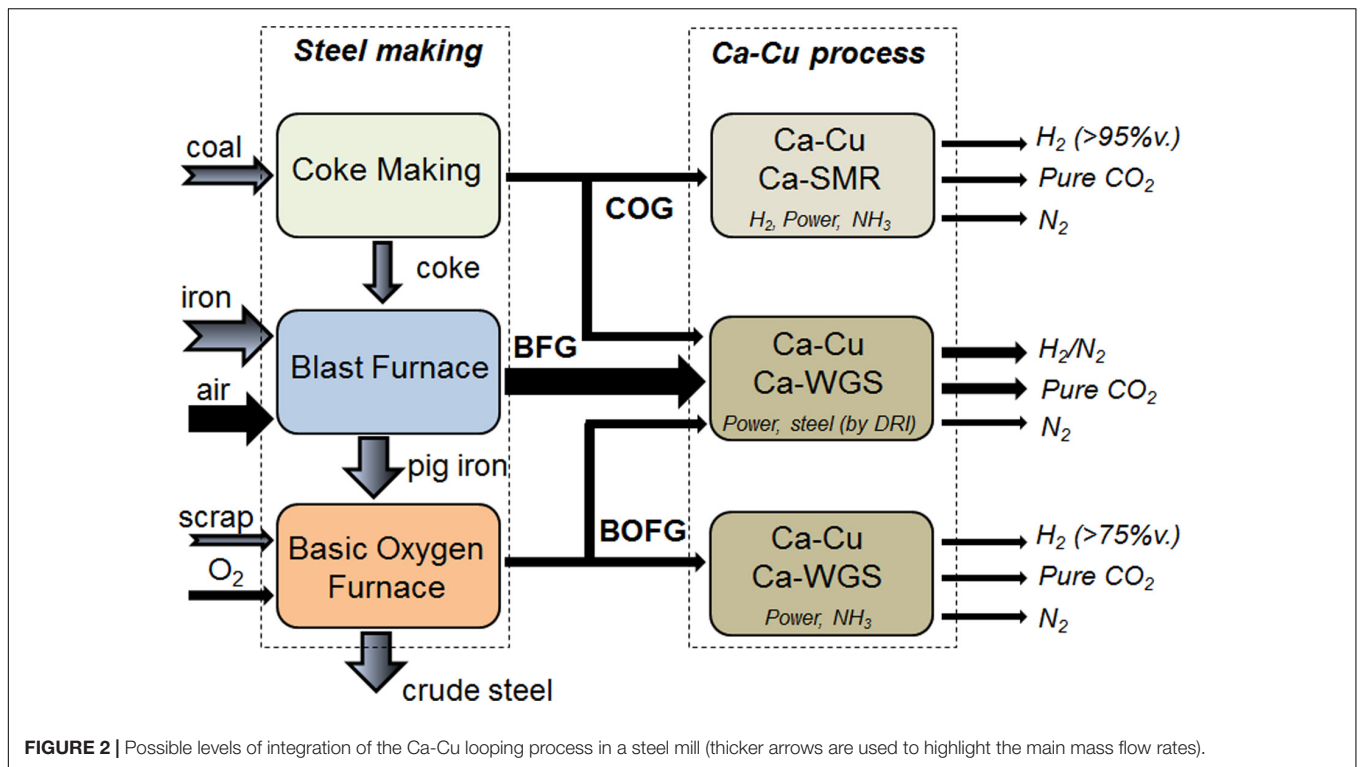|	Blast furnace gas (BFG)	Coke oven gas (COG)	Basic oxygen furnace gas (BOFG)
	Composition (%vol)		
CH_4	–	25	–
CO	23	7	57
CO_2	23	3	15
H_2	4.5	60	2
H_2O	–	–	12
N_2	49.5	5	14
O_2	–	–	–
Flowrate (Nm^3/t of steel)	1630	164	70

FIGURE 2 | Possible levels of integration of the Ca-Cu looping process in a steel mill (thicker arrows are used to highlight the main mass flow rates).
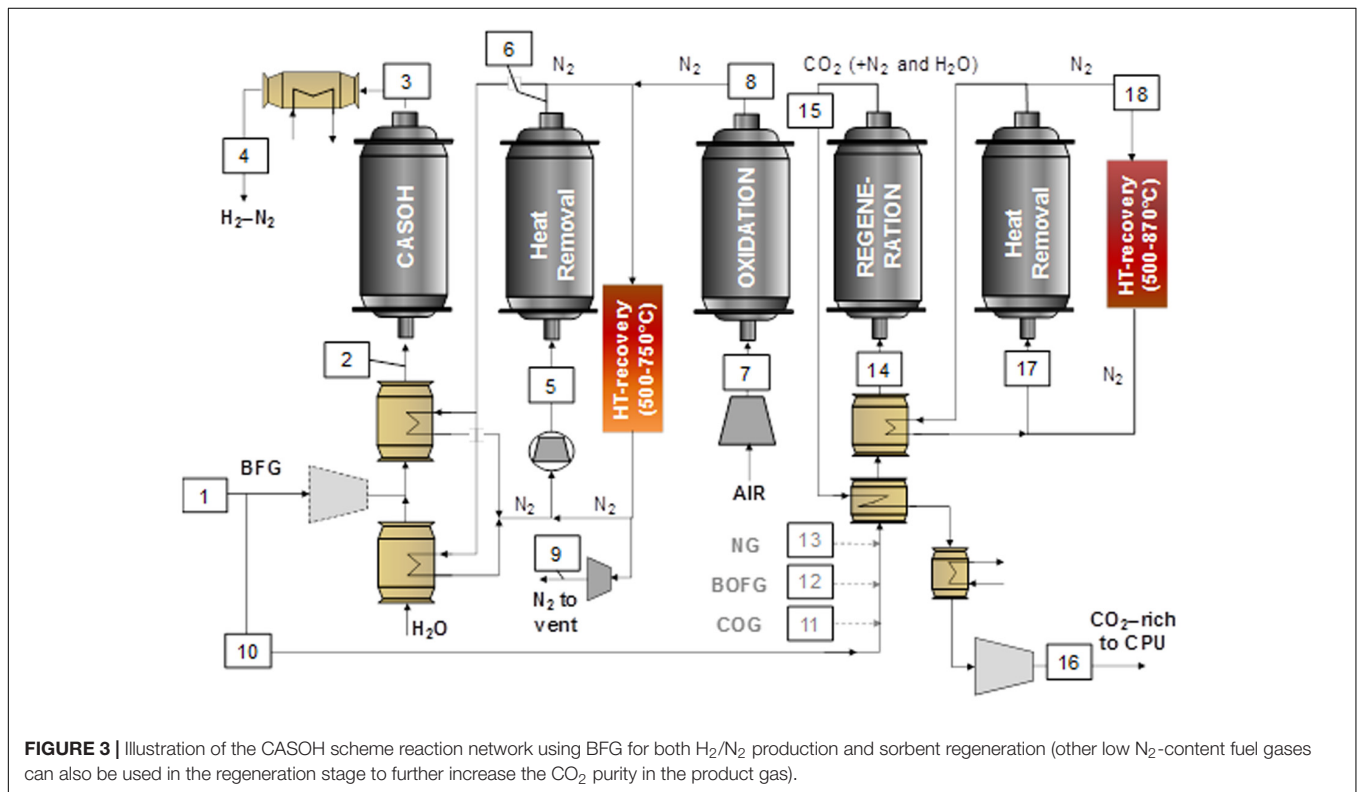

FIGURE 3 | Illustration of the CASOH scheme reaction network using BFG for both H_2/N_2 production and sorbent regeneration (other low N_2-content fuel gases can also be used in the regeneration stage to further increase the CO_2 purity in the product gas).

Figure 4A shows the important role of the CaO sorbent in the thermodynamics of the WGS process. In conventional WGS, a maximum concentration of 40%vol. H_2 (on a N_2-free and dry basis) can be achieved at $550°C$, at atmospheric pressure and with a steam-to-carbon molar ratio of 1. At higher temperatures, the concentration of H_2 is progressively reduced at the expense

FIGURE 4 | (A) Equilibrium of WGS reaction as a function of the temperature with and without CaO-based sorbent; **(B)** effect of pressure on Calcium assisted WGS reaction.
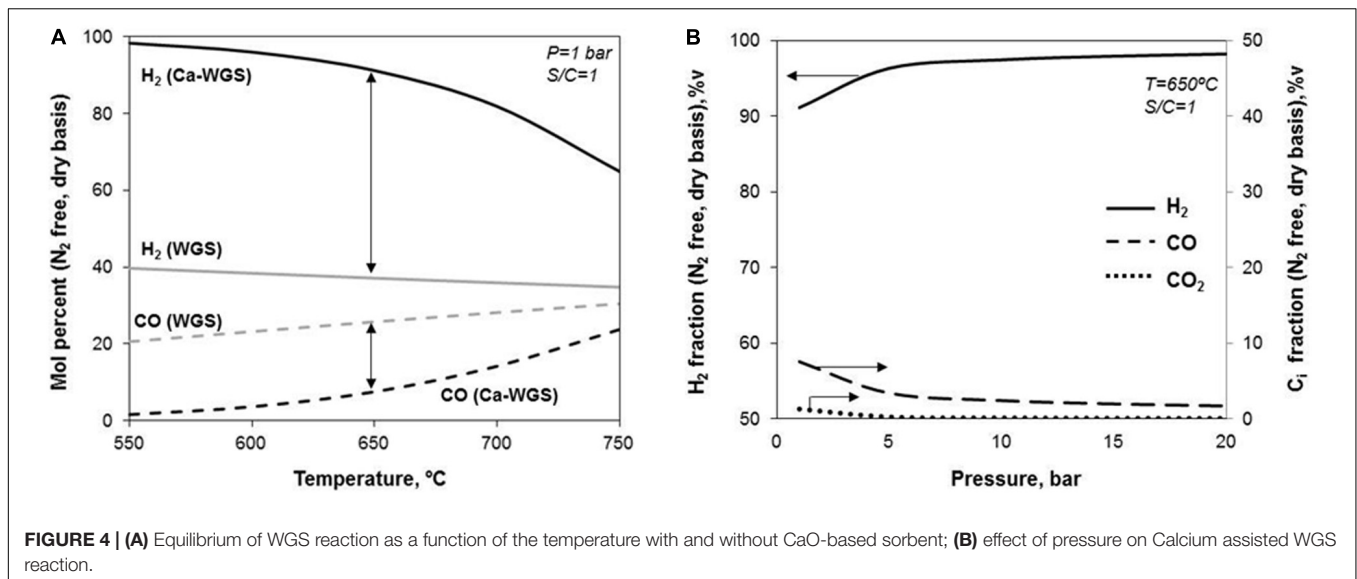
of an increase in the concentration of CO in the product gas from 20%vol. at 550°C to 30%vol. at 750°C. In contrast, when CO_2 is removed from the gas phase by the carbonation of CaO, almost pure H_2 (above 98%vol.) with only 1%vol. of CO (on a dry basis) can be produced at 550°C. The advantages of the Calcium assisted WGS decrease at higher temperatures giving rise to lower concentrations of H_2. At temperatures above 750°C (and at atmospheric pressure), the carbonation of CaO is less favored thermodynamically, and as a result of that, the performance of the Calcium assisted WGS approaches that of standard WGS without CO_2 capture. Taking into account the high content of CO and CO_2 in the BFG and the exothermic nature of both WGS and CaO carbonation reactions ($\Delta H_{298\ K}$ = -41 and -179 kJ/mol, respectively), a great proportion of inert solids (i.e., the materials on which the active CaO and Cu phases are supported) is required in the bed in order to avoid a solid temperature increase and the generation of hot spots during the CASOH stage, that would impede high H_2 yields.

With respect to the effect of the pressure on the Calcium assisted WGS, the production of H_2 is promoted at increasing pressures due to the reduction in the number of gaseous moles associated to the overall reaction (WGS + CaO carbonation). As can be seen in **Figure 4B**, around 90%vol. of H_2 and 8%vol. of CO (on a dry basis) can be achieved working at 650°C, at atmospheric pressure and with a S/C molar ratio of 1 in the feed. However, it is possible to obtain a product gas with a H_2 content of 97%vol., around 3%vol. of CO and a negligible amount of CO_2 performing at 10 bar while maintaining the rest of operating conditions. Since the compression of BFG may be costly, operating the CASOH stage at high pressure may be particularly interesting if part of the energy recovered from the process is used for power generation (i.e., burning the H_2/N_2 gas or producing high-pressure steam) or if the process downstream requires high pressure (i.e., ammonia production). Finally, other important parameter in the Calcium assisted WGS operation is the S/C molar ratio in the feed. As explained in a previous

work (Fernández et al., 2017), almost pure H_2 (on a dry basis) is feasible with moderate steam consumption (i.e., with S/C molar ratios of around 1).

Once the CaO-based particles approach total carbonation with CO_2, the maximum conversion of BFG to H_2/N_2 achieved during the CASOH stage is no longer feasible and the reactor would perform as a stationary WGS unit. It is therefore necessary to add reaction stages to regenerate the sorbent while producing a concentrated stream of CO_2. As can be seen in **Figure 1**, such process requires first a reaction stage in which the Cu-based particles are oxidized to CuO, as their subsequent reduction with a fuel gas will supply the heat needed for the regeneration of the carbonated sorbent. However, by the end of the CASOH operation, the solids bed is left at temperatures up to 700–800°C, which are excessively high to directly initiate the highly exothermic Cu oxidation stage ($\Delta H_{298\ K}$ = -312 kJ/mol O_2). For this reason, an intermediate heat removal stage at high pressure to avoid $CaCO_3$ calcination is included in the process scheme to extract the excess of heat from the solids by flowing through the reactor (stream 6 in **Figure 3**) an inert gas (typically N_2), which also acts as purge for the subsequent oxidation and it can be operated in a semi-closed loop fed into at an appropriate temperature (around 500°C) to start safely with the oxidation of the Cu-based particles.

During the Cu oxidation stage, a flow of air (stream 8 in **Figure 3**) progressively reacts with the metal-based particles and the heat released rapidly increases the temperature of the bed until a maximum value is achieved in the oxidation front. Temperatures close to 800°C allow a fast and complete conversion of O_2 giving as a result a product gas mainly composed of N_2 (stream 9) during the pre-breakthrough period (Alarcón et al., 2017). Moreover, this operation must be carried out preferably at high pressure (i.e., around 10 bar) to minimize the partial calcination of $CaCO_3$ that, would lead to CO_2 slip during this stage. In these mild oxidation conditions, the

chemical stability of the metal oxide is ensured in the long term after successive redox cycles (Adanez et al., 2012) and the raise in temperature required in the next sorbent regeneration stage to achieve values of around 900°C is moderate, which permits reasonable Cu/Ca ratios in the composition of the solids bed.

In the following stage, the CaO-based sorbent is regenerated by *in situ* calcination of $CaCO_3$ ($\Delta H_{298\ K}$ = 171 kJ/mol) when burning a fuel gas containing CO, H_2, and/or CH_4 with the oxygen contained in CuO ($\Delta H_{298\ K}$ = -126.9 kJ/mol CO, $\Delta H_{298\ K}$ = -85.8 kJ/mol H_2, $\Delta H_{298\ K}$ = -178 kJ/mol CH_4). This is equivalent to the operation carried out in typical fuel reactors of chemical looping combustion systems. This stage must be performed at atmospheric pressure to moderate the temperature required for the calcination of $CaCO_3$, according to the $CaO/CaCO_3$ equilibrium (i.e., between 850 and 900°C depending on the concentration of CO_2 in the product gas). Different fuel gases can be used, such as BFG, COG, BOFG, or external natural gas (mostly CH_4), which determines the Cu/Ca ratio required in the bed to sustain the reduction/calcination stage. The use of exclusively BFG as reducing gas avoids the consumption of valuable gases with higher calorific value. However, this option restricts the amount of H_2/N_2 produced through the CASOH operation, as will be explained in the next section. Moreover, CO_2 diluted with N_2 (around 60%vol. CO_2 on a dry basis) is obtained as gaseous product (BFG typically contains concentrations of N_2 close to 50 vol.%), which makes necessary a larger compression and separation unit (CPU) downstream to finally dispatch pure CO_2 for permanent storage or chemical synthesis. The use of COG and BOFG in the regeneration stage allows a higher amount of BFG to be upgraded in the CASOH reactor, and a great decarbonization (about 95%) in the steel plant can be achieved, as these gases end up as highly pure CO_2 and H_2O during the reduction/calcination reactions. However, the availability of COG and BOFG in the plant is limited, thus BFG or external CH_4 must be supplied in this case to accomplish the calcination of the CO_2 sorbent. The use of exclusively CH_4 in the reduction/calcination operation allows all the BFG to be processed in the CASOH stage and simplifies the purification of the CO_2-rich gas obtained in the process, as only CO_2 and H_2O would be produced in the reduction/calcination operation (i.e., only a minimum CO_2 conditioning other than water condensation before compression would be needed). However, this option would involve a great external energy input to the system, so a thorough economical evaluation is required to determine the feasibility of this option.

Once both calcium- and copper-based particles have been totally converted, a large fraction of the solids bed is left at temperatures around 870°C, which are excessively high to carry out an optimal performance of the CASOH stage in a subsequent cycle. Therefore, the heat accumulated in the packed-bed reactor is blown out by flowing through the bed a pressurized stream of recycled inert gas (typically N_2) that enters at a suitable temperature (around 500°C) to begin afterward with the CASOH stage. The gas (stream 18 in **Figure 3**) is discharged at around 870°C, cooled to 500°C and recirculated back to the reactor operated in a closed loop or it can be expanded in a gas turbine for power generation. The exhaust N_2 will be re-compressed and recirculated to the heat removal stages in a similar operation to that carried out in packed-bed chemical looping combustion (CLC) systems (Spallina et al., 2014) or in post-combustion applications where the flue gas is recirculated to increase the CO_2 content in the gas, thereby facilitating the CO_2 capture (Jonshagen et al., 2010).

RESULTS

Reactor Operation
The dynamic performance of the packed-bed reactors in every stage of the proposed process is described in this work by means of a relatively simple reactor model, in which ideal regenerative heat exchange between gas and solids is assumed as well as plug flow without axial dispersion and solid-gas reactions taking place in sharp reaction fronts. These suppositions have been used in previous works to approximate the operation of fixed-bed reactors in CLC (Noorman et al., 2007; Fernández et al., 2012) and catalytic processes (Kolios et al., 2000). Moreover, numerous studies have demonstrated experimentally the veracity of this approach (Kumar et al., 2000; Dupont et al., 2008; Noorman et al., 2010; Spallina et al., 2017).

When the resistance to mass and heat transfer is negligible, the velocity at which the reaction front moves through an adiabatic bed (u_{rf}) can be calculated as follows:

$$u_{rf} = \frac{\rho_{gas} u_{gas} x_{gi} M_{sj}}{\varepsilon \rho_s x_{sj} M_{gi} \varphi} \qquad (1)$$

TABLE 2 | Operating conditions of every stage of the Ca-Cu looping process for the reference case.

Conditions	Value
Solids properties	
Active content in CaO-based solid, %wt.	10
Active content in Cu-based solid, %wt.	30
CASOH stage	
Initial bed temperature, °C	500
Pressure, bar	10
S/C molar ratio	1.2
Inlet gas temperature, °C	500
Cu oxidation stage	
Initial bed temperature, °C	500
Pressure, bar	10
Inlet gas temperature, °C	500
Reduction/calcination stage	
Initial bed temperature, °C	763/500
Pressure, bar	1
Feed temperature, °C	800
Calcination temperature, °C	870
Heat removal stages	
Initial bed temperature (HR1), °C	754/523
Initial bed temperature (HR2), °C	870/800
Pressure, bar	10
Inlet temperature (HR1), °C	523
Inlet temperature (HR2), °C	500

where u_g is the velocity of the gas, ρ_{gas} and ρ_s denote the density of the gas and the solid, respectively, x_{gi} and x_{sj} represent the mass fraction of the reacting component i in the gas and component j in the solid, respectively, M_i is the molecular weight of reacting phases, ε is the bed porosity and φ is the stoichiometric coefficient of the solid/gas reaction. Likewise, the velocity of the heat exchange fronts (u_{he}) advancing along the reactor can be obtained as follows:

$$u_{he} = \frac{\rho_{gas} u_{gas} c_{p,gas}}{\rho_s c_{p,s}} \qquad (2)$$

The maximum temperature change caused by the exothermic or endothermic reactions can be calculated by means of an energy balance assuming adiabatic conditions, according to Eq. (3) and Eq. (4).

$$\Delta T = \frac{\Delta H_r}{\frac{c_{ps} M_{sj}}{x_{sj} \phi} - \frac{c_{pgas} M_{gi}}{x_{gi}}} \qquad \text{if } u_{rf} > u_{he} \qquad (3)$$

$$\Delta T = \frac{\Delta H_r}{\frac{c_{pgas} M_{gi}}{x_{gi}} - \frac{c_{ps} M_{sj}}{x_{sj} \phi}} \qquad \text{if } u_{rf} < u_{he} \qquad (4)$$

A reference case has been studied in detail to demonstrate the feasibility of the process, in which a fraction of the BFG produced in the steel mill is upgraded to H_2/N_2, whereas the rest of this gas is used as sole reducing agent in the sorbent regeneration stage. Both mass and energy balances have been solved for every stage of the process assuming adiabatic reactors. A set of operating conditions and a heat management strategy (explained below) have been adopted to ensure a suitable performance of the reactors. The input of operating conditions adopted in this case are listed in **Table 2**. **Figure 5** shows the evolution of the temperature profiles during the operation in every stage of the process for the conditions assumed in the reference case.

To produce 1 million tons of steel per year, approximately 51.7 Nm³/s of BFG are emitted (Santos, 2013). In the reference case, about 30% of the BFG is directed to the CASOH stage mixed with 4.5 Nm³/s of steam to obtain a steam-to-CO molar ratio of 1.2 in the feed (stream 2 in **Figure 3**). Meanwhile, the remaining 70% of the BFG (stream 10 in **Figure 3**) is used in the sorbent regeneration stage, as explained below. The energy balance in the reduction/calcination stage for the conditions listed in **Table 2** when only BFG is used as fuel imposes a $CuO/CaCO_3$ molar ratio in the bed of 1.4 to ensure that the heat released by the reduction of CuO to Cu is enough to drive the decomposition of $CaCO_3$ to CaO. **Table 3** includes the flow rates, temperatures and compositions of the gaseous streams calculated for this case.

In these conditions, when the CASOH stage starts the bed will contain 66%wt of Ca-based material (with 7%wt of active CaO, according to the solids properties listed in **Table 2**) and 34%wt of Cu-based particles (i.e., 10%wt of Cu supported over 24 wt% of SiO_2). To carry out the CASOH stage, the mixture of BFG and steam is compressed up to 10 bar and subsequently preheated up to approximately 500°C. Moreover, the solids in the bed are initially at 500°C as a result of a previous heat removal stage. This temperature should allow

a very fast reaction of CO with H_2O to form CO_2 and H_2 catalyzed by the Cu-based particles. According to the reactor model explained above, a slight increase in the solids temperature of 23°C is produced due to the modest exothermicity of the WGS reaction. At 523°C, 10 bar and a S/C molar ratio of 1.2, the WGS equilibrium predicts a CO conversion of around 80%. CO_2 is assumed to be removed as soon as the product gas contacts with active calcium oxide, which increases the conversion of CO. Thus, a carbonation front is formed and moves ahead at a velocity (u_{rf}) that can be calculated by means of Eq. (1). Considering the composition of both reacting gas and solids, the carbonation front advances near 6 times faster than the resulting heat exchange front (i.e., $u_{rf} > u_{he}$) and leaves behind carbonated solids (and Cu-based particles) heated by the carbonation reaction. For the conditions of the reference case, a maximum temperature of 754°C (Eq. 3) is achieved in the heat plateau developed between both reaction and heat exchange fronts. At this temperature, it is possible to obtain a product gas (stream 3) with 32% H_2, 60% N_2 and less than 2% of CO and CO_2 (see **Table 3**).

Because of the rapid heat transfer between the gas and solids, the product gas acquires the temperature of the unconverted solids downstream and it is delivered at 500°C during the entire CASOH stage. A flow of 13.5 Nm³/s of decarbonized H_2/N_2 gas is obtained, which can be used to cover energy requirements of the steel mill (as happens with BFG and other off-gases in conventional plants without CO_2 capture), to generate power or to produce additional steel by means of a DRI process avoiding carbon emissions. The integration of these uses of the H_2/N_2 stream is beyond the scope of this work. Assuming that the H_2 contained in stream 3 (i.e., 4.32 Nm³/s) was able to fully reduce iron ore (Fe_2O_3) in a parallel DRI process, about 0.23 Mt/year of steel would be produced additionally in the steel plant (i.e., 23% of increased production).

When the carbonation front approaches the reactor exit, all the active CaO (i.e., 10%wt of the calcium-based material) has been carbonated and the CASOH stage concludes. At this point, near 80% of the solids are ideally left at 754°C and the rest of the bed at 523°C, as a result of the advance of the heat exchange front resulting from the carbonation reaction (see **Figure 4**).

Once the CASOH stage has finished, the fact that a large fraction of the reactor is left at around 750°C makes it necessary the addition of a heat removal stage to eliminate the excess of heat absorbed in the bed before starting the highly exothermic copper oxidation stage. An inlet flow of 157 Nm³/s of N_2 (stream 5 in **Figure 3**) allows this operation to be carried out in the same cycle time than the CASOH stage. This stream comes recirculated and re-compressed from a high-temperature recovery system (see **Figure 3**) and it is fed at 523°C through the part of the reactor at lower temperature. As the N_2 goes through the bed, the heat exchange front located in the transition between the zones at 523/754°C gradually moves toward the reactor exit, whereas the outlet gas (stream 6 in **Figure 3**) is released at 754°C. The heat recovered from the exit gas can be used to supply heat to other unit of the steelwork (e.g., partly pre-heating a reheating oven) or it can be recovered to produce HP steam for additional power generation. In this way, N_2 is operated in
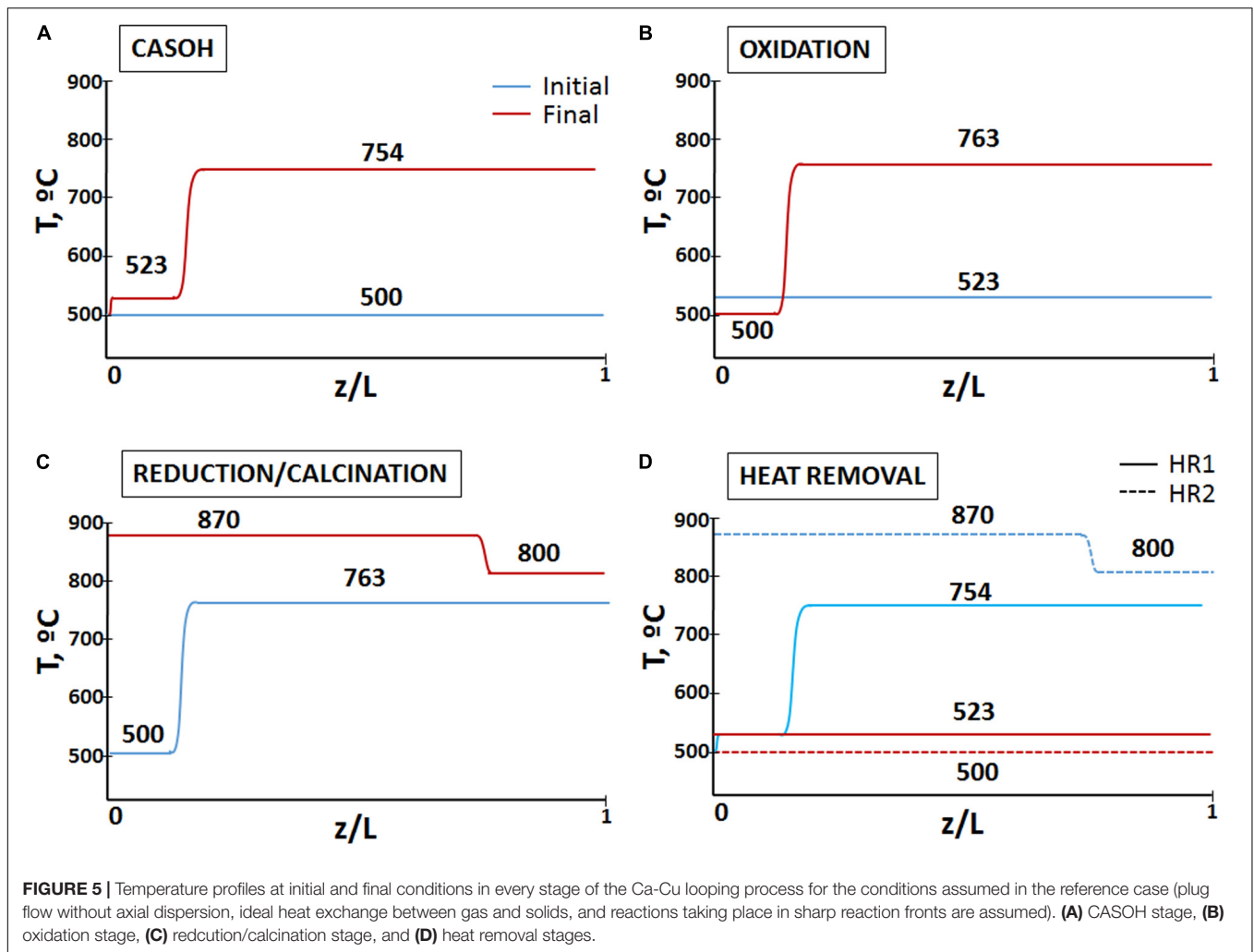
FIGURE 5 | Temperature profiles at initial and final conditions in every stage of the Ca-Cu looping process for the conditions assumed in the reference case (plug flow without axial dispersion, ideal heat exchange between gas and solids, and reactions taking place in sharp reaction fronts are assumed). **(A)** CASOH stage, **(B)** oxidation stage, **(C)** redcution/calcination stage, and **(D)** heat removal stages.

TABLE 3 | Main characteristics of the gaseous streams of the Ca-Cu looping process (see **Figure 3**) obtained by solving the mass and energy balances in the reference case.

Stream	1	2	3	4	5	6	7	8	9	14	15	16	17	18
Flow, Nm^3/s	51.7	20.7	13.5	12.7	156.9	156.9	23.3	18.6	18.6	35.5	42.5	40.9	179.3	179.3
Flow, kmol/s	2.3	0.9	0.6	0.6	7.0	7.0	1.0	0.8	0.8	1.6	1.9	1.8	8.0	8.0
Flow, kg/s	70.4	25.7	11.6	10.9	196.1	196.1	30.0	23.4	23.4	48.4	69.1	67.8	224.1	224.1
T, °C	25.0	488.1	500.0	25.0	523.0	754.0	500.0	523.0	116.0	800.0	500.0	30.0	500.0	851.5*

						Composition, %vol.								
CH$_4$	–	–	–	–	–	–	–	–	–	–	–	–	–	–
CO	23	18	1	1	–	–	–	–	–	23	–	–	–	–
H$_2$	4.5	3.5	32.1	34	–	–	–	–	–	4.5	–	–	–	–
CO$_2$	23	18	1	1	–	–	–	1.1	1.1	23	54.9	57.1	–	–
H$_2$O	–	21.6	6.5	–	–	–	–	–	–	–	3.8	–	–	–
O$_2$	–	–	–	–	–	–	21	–	–	–	–	–	–	–
N$_2$	49.5	38.9	59.5	64.0	100	100	79	98.9	98.9	49.5	41.3	42.9	100.0	100.0

*Average temperature during the duration of the stage.

a closed loop cycle in which only a small make up is required to account for the amount of gas used as purge gas. This stage ends when all the heat stored at 754°C is blown out of the bed.

At this point, the solids bed is left at a uniform and sufficiently high temperature (i.e., 523°C) to initiate the subsequent Cu oxidation operation.

During the Cu oxidation, a flow of air of 23.3 Nm³/s (stream 7 in **Figure 3**) is required to adapt the duration of this stage to the previous ones. The inlet gas is supplied at 10 bar and 500°C. According to the solid compositions listed in **Table 2**, the reactor contains 10%wt of Cu at the beginning of the Cu oxidation stage. In these conditions, the oxidation front goes through the bed around 9 times faster than the corresponding heat exchange front, according to Eq. (1) and Eq. (2), and the maximum increase in temperature in the oxidation front is 240°C, calculated by means of Eq. (3).

The rapid advance of the oxidation front facilitates that the solids bed reaches a maximum temperature of 763°C. An operating pressure of 10 bar ensures a very low leakage of CO_2 caused by partial calcination of $CaCO_3$ ($P_{CO2,eq}$ at 763°C is 0.11 bar). The high temperature achieved in the oxidation front permits the complete conversion of the oxygen, giving as a result an outlet flow of 18.6 Nm³/s basically composed of N_2 (with only 1.1%vol of CO_2), which is discharged at 523°C. Once the Cu present in the reactor has been totally oxidized, the bed is divided into two zones at different temperature as a consequence of the advance of both oxidation and heat exchange fronts at different velocities. A small fraction of the solids located close to the reactor inlet (around 10% of the solids bed) remains at 500°C (i.e., the temperature of inlet air) and the remaining 90% of the reactor is left at 763°C.

As mentioned above, for the conditions of the reference case, about 70% of the BFG is needed to regenerate the CO_2 sorbent carbonated in the CASOH stage. Moreover, the pressure must be reduced close to atmospheric conditions to favor the calcination reaction at temperatures below 900°C. In this case, the operation is carried out with a flow of 35.5 Nm³/s of BFG°C, which enters preheated at 800°C (stream 14 in **Figure 3**). This high temperature allows the fast reduction of CuO with the CO and H_2 contained in the BFG and avoids the re-carbonation of the calcium-based particles left behind the heat exchange front generated by the reduction/calcination reactions (see **Figure 5C**). Under these circumstances, the temperature of the solids in the reduction front rapidly increases until a value of 870°C is achieved. The composition of both solids bed and BFG makes the reduction front move through the reactor around 4 times faster than the resulting heat exchange front leaving behind a heat plateau at 870°C. This temperature should be sufficient to ensure the complete calcination of the sorbent ($P_{CO2eq, 870°C}$ = 0.65), taking into account that the maximum concentration of CO_2 expected in the product gas is 55%vol, assuming total oxidation of the BFG. Downstream of the reduction front, the product gas rapidly reaches the temperature of the unconverted solids and it is discharged at 500°C. The concentrated stream of CO_2 (stream 16 in **Figure 3**) needs an additional purification step before being ready for use or storage, but the analysis of such purification options (physical absorption, cryogenic distillation, membrane separation, adsorption, etc.) is outside the scope of this work. As mentioned above, fuel gases without N_2 would be preferable to minimize the footprint of such purification stage.

Once the reduction/calcination operation has finished, around 75% of the bed remains at 870°C and the rest of the reactor is left at 800°C. As explained above, the CASOH stage requires much lower temperatures, so the excess of heat stored in the bed is recovered by feeding into N_2 at high pressure in a similar manner to the previous heat removal stage. Therefore, a flow of 179.3 Nm³/s of N_2 at 10 bar and 500°C (stream 17 in **Figure 3**) enters the reactor and the exit gas containing high-temperature heat can be used to cover energy demand in other part of the plant or used to produce high-pressure steam for the generation of power in a steam turbine. During approximately 75% of the duration of the heat removal operation, the N_2 stream is emitted at 870°C and the rest of the time it is discharged at 800°C (i.e., an average temperature of the exit gas of 852°C). This stage culminates when the bed is left at 500°C (i.e., the temperature chosen to start the CASOH stage in a subsequent cycle).

There are other alternatives to increase the amount of H_2/N_2 obtained from BFG through the Ca-Cu looping process. If the COG and BOFG are also used as reducing gases to regenerate the Ca-based sorbent (together with BFG to cover the energy requirements of the operation), a higher proportion of BFG can be converted into H_2-enriched gas in the CASOH stage (Case 2 in **Table 4**). In this particular configuration, around 45% of the BFG available from the steel mill can be upgraded (i.e., 22.9 Nm³/s and around 40% of additional H_2-rich stream compared to the previous case) via the Calcium assisted WGS process described above. With this option, almost the complete decarbonization of the steel plant is feasible, as most of the carbon present in the steel mill off-gases is finally emitted in the CO_2-rich gas produced in the reduction/calcination stage. Moreover, the purification of the CO_2 is facilitated as the product gas resulting from the regeneration stage contains a higher concentration of CO_2 (i.e., 64%vol. on a dry basis).

If CH_4 is used as fuel in the reduction/calcination stage, all the BFG produced during the steelmaking process can be directed to the CASOH stage (Case 3 in **Table 4**), thereby maximizing the production of H_2/N_2 (i.e., 42.3 Nm³/s). In these conditions, the purification of CO_2 is greatly simplified because only CO_2 and $H_2O_{(v)}$ are produced during the regeneration. However, this option demands a large energy input to the Ca-Cu looping process (i.e., 20.3 Nm³/s of CH_4 equivalent to 594 MW_{th}) to decarbonize all the BFG (i.e., with a calorific value of around 181 MW_{th}, assuming LHV_{BFG} = 2.6 MJ/kg). Moreover, the lower enthalpy of the reduction reaction with CH_4 imposes a larger Cu/Ca molar ratio in the bed (i.e., a value of 4.2 in this specific case), which results in significantly larger reactors to treat the same flow of BFG. The higher proportion of Cu in the bed (15%wt in this case) shoots up the temperature in the oxidation front until 870°C, which highly increases the loss of CO_2 by partial calcination of $CaCO_3$ in this stage (even operating at 15 bar as in Case 4 of **Table 4**), and consequently, the CO_2 capture efficiency of the process decreases to around 85%.

Integration in the Steel Mill

The overall process performance of the cases discussed above are summarized in this section. The preliminary energy analysis is based on the following assumptions:

TABLE 4 | Main performance results of different configurations of the Ca-Cu process fueled with steel mill off-gases.

		Case 1 Only BFG	Case 2 BFG/COG/BOF	Case 3 BFG/NG	Case 4 BFG/NG
CASOH operating P	Bar	10	10	10	15
Thermal input, BFG	$MW_{LHV,BFG}$	175.07	175.07	175.07	175.07
Flowrate, BFG	kmol/s	2.31	2.31	2.31	2.31
Thermal input, COG	$MW_{LHV,COG}$	–	84.80	–	–
Flowrate, COG	kmol/s	–	0.23	–	–
Thermal input, BOFG	$MW_{LHV,BOF}$	–	16.44	–	–
Flowrate, BOFG	kmol/s	–	0.10	–	–
Thermal input, NG	$MW_{LHV,NG}$	–	–	594.0	594.0
Flowrate, NG (100% CH_4)	kmol/s	–	–	0.74	0.74
Thermal output, H_2/N_2	$MW_{LHV,H2-rich}$	48.44	68.14	153.64	153.62
Flowrate, dry	kmol/s	0.57	0.80	1.79	1.79
Composition, dry	$H_2/N_2/CO_x$	34/64/2	34/64/2	35/64/1	35/64/1
CO_2 purity, dry (before CPU)	%	57.0%	64.1%	99.8%	99.9%
CO_2 emitted	%	2.0%	4.2%	20.4%	15.9%
Cold gas efficiency	%	27.7%	24.7%	20.0%	20.0%
Electric utilities	MW_{el}	48.3	55.7	82.7	95.8
Heat recovery (500–200°C)	MW_{th}	18.5	20.2	22.9	24.1
Heat recovery (870–500°C)	MW_{th}	98.5	176.2	577.3	583.4
Energy efficiency	%	74.1%	79.7%	88.5%	88.0%
Primary energy efficiency	%	69.8%	77.6%	90.5%	89.2%
Specific energy consumption for CO_2 removed	MJ_{LHV}/kg_{CO2}	1.68	1.62	1.37	1.50

Heat Recovery

Two different heat recovery units are considered to distinguish the quality of the heat. The high-temperature heat (i.e., in the range from 500 to 870°C) can be used to supply heat directly in some point of the steel mill, thereby reducing the energy demand of the integrated steelworks, as well as for the production of high-pressure steam for power generation. Moreover, part of this heat is also needed to preheat the fuel fed into the regeneration stage up to 800°C. On the other hand, the intermediate-temperature heat (i.e., between 200 and 500°C), which is mainly obtained from the cooling of product gases, can be used to preheat gaseous feedstock, to produce the steam required in the CASOH process and to produce additional intermediate-pressure (IP) steam for thermal and electricity generation.

Electric Utilities

If the power generation from burning the H_2/N_2 obtained during CASOH is not considered, the Ca-Cu looping process has some electricity demand to operate the compressors of the plant, in particular those needed to feed BFG for CASOH, air for the Cu oxidation and the CO_2-rich stream obtained in the regeneration stage that must be sent (compressed up to 80 bar) to the CO_2 Purification Unit (CPU). However, a small fraction of electricity is recovered by expanding the flue gas from the oxidation stage to the atmosphere.

CO$_2$ Emissions

Most of the CO_2 emitted to the atmosphere is produced by partial calcination of $CaCO_3$ during the oxidation stage. This number can increase depending on the separation efficiency of the CO_2

purification unit (likely > 90%) except for the cases 3 and 4, where virtually pure CO_2 is directly obtained (after H_2O_v condensation) from the regeneration reactor. The efficiency of the separation also depends on the CO_2 purity at the regeneration step.

Table 4 summarizes the thermodynamic performance of all the proposed Ca-Cu looping configurations. The energy content of the H_2/N_2 fuel production is calculated with the cold gas efficiency (CGE) by means of Eq. (5):

$$CGE = \frac{\dot{m}_{H_2\ rich}LHV_{H_2\ rich}}{\sum \dot{m}_i LHV_i}; i : BFG, COG, BOFG, NG \quad (5)$$

where i can be BFG, COG, BOFG, NG, m is the mass flow rate and LHV the corresponding low heating value of the fuels. The overall energy efficiency (η_E) is obtained assuming for the inlet and outlet energy streams of the process the same quality as follows:

$$\eta_E = \frac{\dot{m}_{H_2\ rich}LHV_{H_2\ rich} + H_{>500°C} + H_{>200°C}}{\sum \dot{m}_i LHV_i + E_{el}} \quad (6)$$

The primary energy efficiency (η_{PE}) is calculated by means of Eq. (7) assuming that the energy conversion in a boiler has an efficiency of 0.9 and the electricity generated in a combined cycle shows an efficiency of 0.6.

$$\eta_{PE} = \frac{\dot{m}_{H_2\ rich}LHV_{H_2\ rich} + \frac{H_{>500°C}+H_{>200°C}}{0.9}}{\sum \dot{m}_i LHV_i + \frac{E_{el}}{0.6}} \quad (7)$$

Finally, it has been calculated the specific energy consumption for CO_2 removed (λ_{CO2}), which measures the primary energy consumption related to CO_2 captured. This coefficient is

conceptually similar to the SPECCA (Specific Primary Energy Consumption for CO_2 Avoided) coefficient conventionally used to compare different CO_2 capture technologies with respect to a benchmark process (Spallina et al., 2017), and it provides valuable quantitative information about the feasibility of the separation process according to Eq. (8).

$$\lambda_{CO_2} \left[\frac{MJ_{LHV}}{kg_{CO_2}} \right] = \frac{\sum \dot{m}_i LHV_i + \frac{E_{el}}{0.6} - \dot{m}_{H_2 \, rich} LHV_{H_2 \, rich} - \frac{H_{>500°C} + H_{>200°C}}{0.9}}{\dot{m}_{CO_2, \, equivalent \, in} - \dot{m}_{CO_2, \, emitted}}$$

(8)

The results indicate that the capacity to convert BFG into H_2/N_2 is limited to around 30% due to the high fuel requirement during the regeneration stage, which is no longer available as chemical energy. However, the high-temperature heat available results very promising since the quality and accessibility can be exploited in several other application including internal uses within the steelworks. In general, the energy efficiency (η_E) is higher than 75%, reaching maximum values around 88% in case of using natural as fuel gas for regeneration. Low values for the specific energy consumption of around 1.5 MJ_{LHV}/kg_{CO_2} demonstrates that the proposed process offers great CO_2 capture rates with moderate energy penalty. The main difference between cases 1–2 and cases 3–4 is the purity at which the CO_2 is delivered after the regeneration stage. The significantly lower N_2 content in the CO_2-rich gas in cases 3 and 4 also decreases the cost of compression (up to 80 bar) to feed the CPU, resulting in higher energy efficiencies and reduced specific consumption for the separation of CO_2. Depending on the CO_2 purification route used in case 1 and case 2, the electric and thermal duty may vary significantly. Despite the overall higher energy performance obtained in the case 3 and case 4, this options are penalized in terms of CGE and higher CO_2 leakage (i.e., hot spots generated during the oxidation stage in beds loaded with higher content of Cu), which may result relevant in terms of economic performance and CO_2 capture efficiency.

CONCLUSION

A process design has determined the operating windows for a Ca-Cu looping process designed to obtain H_2-rich gas from BFG with CO_2 capture. The resulting decarbonized fuel gas can be used for onsite power generation or to obtain sponge iron by a DRI process, increasing the overall capacity of the plant. A large amount of high-temperature heat (up to 870°C) is also produced, which is suitable for covering heat demand of the steel mill or for power generation. Several configurations of the Ca-Cu looping process involving different fuel gases for the regeneration stage are technically viable in terms of process operating conditions and fuel utilization. The performance for every case has been compared in terms of primary energy consumption, product yields, CO_2 purity and potential CO_2 capture rate. Preliminary energy and mass balances of the process indicate that around 30% of the BFG can be upgraded via calcium assisted WGS if only BFG is used as reducing gas in the reduction/calcination stage.

The maximum temperature achieved during the Cu oxidation stage can be maintained below 760°C, resulting in a negligible calcination of the $CaCO_3$ present in the bed. The regeneration stage carried out with the remaining 70% of the BFG gives as a result a product gas with 55%v. of CO_2 diluted in N_2, which needs a subsequent CO_2 purification step in a CPU. An energy efficiency of 74% for this option has been calculated together with a CO_2 capture efficiency of 98%. When the COG and BOFG available in the steel mill are used as reducing gases (together with BFG to cover the energy requirements of the operation), about 45% of the BFG can be upgraded giving as a result around 40% of additional H_2-rich stream compared to the previous case. An energy efficiency of 80% for this case is obtained together with a CO_2 capture efficiency of 95%. CO_2 purification is less demanding as the product gas from the regeneration stage contains a higher concentration of CO_2 (i.e., 64%vol. on a dry basis). When natural gas is used as fuel for sorbent regeneration, all the BFG can be directed to the CASOH stage, thereby maximizing the production of H_2/N_2. In these conditions, the purification of CO_2 is much easier as only CO_2 and $H_2O_{(v)}$ are produced during the regeneration stage. This option demands a large energy input to decarbonize all the BFG (i.e., around 600 MW_{th} of methane to upgrade 180 MW_{th} of BFG). However, most of the energy can be recovered as high-temperature heat resulting an energy efficiency for this option around 90%. The lower reduction enthalpy of CuO with CH_4 imposes higher copper content in the bed, which causes high temperatures during Cu oxidation, and therefore, higher CO_2 leakage resulting in a lower CO_2 capture efficiency of 80%. A higher pressure of 15 bar during Cu oxidation allows an improved CO_2 capture efficiency of 85%. In general, low values for the specific energy consumption between 1.4 and 1.7 MJ_{LHV}/kg_{CO_2} have been calculated, which demonstrates the potential of this process to obtain H_2/N_2 gas and pure CO_2 from BFG with moderate energy penalty.

DATA AVAILABILITY STATEMENT

The raw data supporting the conclusions of this article will be made available by the authors, without undue reservation, to any qualified researcher.

AUTHOR CONTRIBUTIONS

JF carried out the process design and developed the basic reactor modeling. VS carried out the integration of the different Ca-Cu configurations in the steel mill. JA contributed to the process design, the discussion of the results, and revised the manuscript. All authors contributed to the article and approved the submitted version.

FUNDING

REFERENCES

Adanez, J., Abad, A., Garcia-Labiano, F., Gayan, P., and de Diego, L. F. (2012). Progress in chemical looping combustion and reforming technologies. *Prog Energy Combust.* 38, 215–282. doi: 10.1016/j.pecs.2011.09.001

Alarcón, J. M., and Fernández, J. R. (2015). CaCO3 calcination by the simultaneous reduction of CuO in a Ca/Cu chemical looping process. *Chem Eng Sci.* 137, 254–267. doi: 10.1016/j.ces.2015.06.030

Alarcón, J. M., Fernández, J. R., and Abanades, J. C. (2017). Study of a Cu-CuO chemical loop for the calcination of CaCO3 in a fixed bed reactor. *Chem. Eng. J.* 325, 208–220. doi: 10.1016/j.cej.2017.05.070

Antzara, A., Herecleous, E., Bukur, D. B., and Lemonidou, A. A. (2015). Thermodynamic analysis of hydrogen production via chemical looping steam methane reforming coupled with in situ CO2 capture. *Int. J. Greenh. Gas Con.* 32, 115–128. doi: 10.1016/j.ijggc.2014.11.010

Arasto, A., Tsupari, E., Karki, J., Pisila, E., and Sorsamaki, L. (2013). Post-combustion capture of CO2 at an integrated steel mill – Part I: technical concept analysis. *Int. J. Greenh. Gas. Con.* 16, 271–277. doi: 10.1016/j.ijggc.2012.08.018

ArcelorMittal (2019). *Climate Action Report 1, Luxembourg*. Available at: https://corporate.arcelormittal.com/media/press-releases/arcelormittal-publishes-first-climate-action-report (accessed February 18, 2020).

Bechara, R., Hamadeh, H., Mirgaux, O., and Patisson, F. (2018). Optimization of the iron ore direct reduction process through multiscale process modeling. *Materials* 11, 1094–1112.

Blamey, J., Anthony, E. J., Wang, J., and Fennell, P. S. (2010). The calcium looping cycle for large-scale CO2 capture. *Prog. Energ. Combus. Sci.* 36, 260–279. doi: 10.1016/j.pecs.2009.10.001

Boon, J., Cobden, P. D., van Dijk, H. A. J., and van Sint Annaland, M. (2015). High-temperature pressure swing adsorption cycle design for sorption-enhanced water-gas shift. *Chem. Eng. Sci.* 122, 219–231. doi: 10.1016/j.ces.2014.09.034

Cavaliere, P. (2019). *Clean Ironmaking and Steelmaking Processes Efficient Technologies for Greenhouse Emissions Abatement*. Switzerland: Springer Nature.

Díez-Martín, L., López, J. M., Fernández, J. R., Martínez, I., Grasa, G., and Murillo, R. (2018). Complete Ca/Cu cycle for H2 production via CH4 sorption enhanced reforming in a lab-scale fixed bed reactor. *Chem. Eng. J.* 350, 1010–1021. doi: 10.1016/j.cej.2018.06.049

Dreillard, M., Broutin, P., Briot, P., Huard, T., and Lettat, A. (2017). Application of the DMX CO2 capture process in steel industry. *Energy Procedia* 114, 2573–2589. doi: 10.1016/j.egypro.2017.03.1415

Dupont, V., Ross, A. B., Knight, E., Hanley, I., and Twigg, M. V. (2008). Production of hydrogen by unmixed steam reforming of methane. *Chem. Eng. Sci.* 63, 2966–2979. doi: 10.1016/j.ces.2008.02.015

Erans, M., Manovic, V., and Anthony, E. J. (2016). Calcium looping sorbents for CO2 capture. *Appl. Energ.* 180, 722–742. doi: 10.1016/j.apenergy.2016.07.074

Fernández, J. R., and Abanades, J. C. (2017a). Optimized design and operation strategy of a Ca- Cu chemical looping process for hydrogen production. *Chem. Eng. Sci.* 166, 144–160. doi: 10.1016/j.ces.2017.03.039

Fernández, J. R., and Abanades, J. C. (2017b). Overview of the Ca–Cu looping process for hydrogen production and/or power generation. *Curr. Opin. Chem. Eng.* 17, 1–8. doi: 10.1016/j.coche.2017.04.010

Fernández, J. R., Abanades, J. C., Murillo, R., and Grasa, G. (2012). Conceptual design of a hydrogen production process from natural gas with CO2 capture using a Ca-Cu chemical loop. *Int. J. Greenh. Gas Con.* 6, 126–141. doi: 10.1016/j.ijggc.2011.11.014

Fernández, J. R., Martínez, I., Abanades, J. C., and Romano, M. C. (2017). Conceptual design of a Ca–Cu chemical looping process for hydrogen production in integrated steelworks. *Int. J. Hydrogen Energ.* 42, 11023–11037. doi: 10.1016/j.ijhydene.2017.02.141

Gazzani, M., Romano, M. C., and Manzolini, G. (2015). CO2 capture in integrated steelworks by commercial-ready technologies and SEWGS process. *Int. J. Greenh Gas. Contr.* 41, 249–267. doi: 10.1016/j.ijggc.2015.07.012

Grasa, G., Navarro, M. V., Lopez, J. M., Diez-Martín, L., Fernandez, J. R., and Murillo, R. (2017). Validation of the H2 production stage via SER under relevant conditions for the Ca/Cu reforming process practical application. *Chem. Eng. J.* 324, 266–278. doi: 10.1016/j.cej.2017.04.134

Harrison, D. P. (2008). Sorption-enhanced hydrogen production: a review. *Ind. Eng. Chem. Res.* 47, 6486–6501. doi: 10.1021/ie800298z

Hills, A. W. D. (1967). Equilibrium decomposition pressure of calcium carbonate between 700 and 900 °C. *Bull. Inst. Min. Met.* 76C, 241–245.

Ho, M. T., Bustamante, A., and Wiley, D. E. (2013). Comparison of CO2 capture economics for iron and steel mills. *Int. J. Greenh. Gas. Contr.* 19, 145–159. doi: 10.1016/j.ijggc.2013.08.003

IEA Report (2017). *Energy Technology Perspectives: Catalysing Energy Technology Transformations*. Paris: International Energy Agency.

IEA Report (2019). *The Future of Hydrogen: Seizing today's opportunities*. France: International Energy Agency.

IEAGHG (2013). *Overview of the Current State and Development of CO2 Capture Technologies in the Ironmaking Process, 2013/TR3*. Cheltenham: IEAGHG.

IPCC (2018). *Global Warming of 1.5°C. An IPCC Special Report on the Impacts of Global Warming of 1.5°C Above Pre-Industrial Levels and Related Global Greenhouse Gas Emission Pathways, in the Context of Strengthening the Global Response to the Threat of Climate Change, sustainable Development, and Efforts to Eradicate Poverty*. Geneva: IPCC.

Ji, G., Yao, J. G., Clough, P. T., Diniz da Costa, J. C., Anthony, E. J., Fennell, P. S., et al. (2018). Enhanced hydrogen production from thermochemical processes. *Energ. Env. Sci.* 11, 2647–2672.

Jin, P., Jiang, Z., Bao, C., Hao, S., and Zhang, X. (2015). The energy consumption and carbon emission of the integrated steel mill with oxygen blast furnace. *Resour. Conserv. Recycl.* 117, 58–65. doi: 10.1016/j.resconrec.2015.07.008

Jonshagen, K., Sipocz, N., and Genrup, M. (2010). A novel approach of retrofitting a combined cycle with post combustion CO2 capture. *J. Eng. Gas Turbines Power* 133, 011703–011710.

Kazi, S. S., Aranda, A., di Felice, L., Meyer, J., Murillo, R., and Grasa, G. (2017). Development of Cost effective and high performance composite for CO2 Capture in Ca-Cu looping process. *Energy Procedia* 114, 211–219. doi: 10.1016/j.egypro.2017.03.1163

Kolios, G., Frauhammer, J., and Eigenberger, G. (2000). Autothermal fixed-bed reactor concepts. *Chem. Eng. Sci.* 55, 5945–5967. doi: 10.1016/s0009-2509(00)00183-4

Kumar, R. V., Lyon, R. K., and Cole, J. A. (2000). "Unmixed reforming: a novel authothermal cycling steam reforming process," in *Advances in Hydrogen Energy*, eds C. E. Gregoire Pedro and F. W. Laurent (Higham, MA: Kluwer Academic Publishers).

Lacroix, M., Broutin, P., Lethier, S., Nevicato, D., Petetin, B., De Coninck, E., et al. (2019). "DMX demonstration in dunkirk: 3D projects granted by H2020: scope and objectives," in *TCCS-10 Conference, Trondheim*, Norway.

Martavaltzi, C. S., Pampaka, E. P., Korkakaki, E. S., and Lemonidou, A. A. (2010). Hydrogen Production via steam reforming of methane with simultaneous CO2 capture over CaO-Ca12Al14O33. *Energy Fuels* 24, 2589–2595. doi: 10.1021/ef9014058

Martínez, I., Armaroli, D., Gazzani, M., and Romano, M. C. (2017). Integration of the Ca–Cu process in ammonia production plants. *Ind. Eng. Chem. Res.* 56, 2526–2539. doi: 10.1021/acs.iecr.6b04615

Martínez, I., Fernández, J. R., Abanades, J. C., and Romano, M. C. (2018). Integration of a fluidized bed Ca–Cu chemical looping process in a steel mill. *Energy* 163, 570–584. doi: 10.1016/j.energy.2018.08.123

Martínez, I., Fernandez, J. R., Martini, M., Gallucci, F., van Sint Annaland, M., Romano, M. C., et al. (2019a). Recent progress of the Ca-Cu technology for decarbonisation of power plants and carbon intensive industries. *Int. J. Greenh. Gas Con.* 85, 71–85. doi: 10.1016/j.ijggc.2019.03.026

Martínez, I., Martini, M., Riva, L., Gallucci, F., Van Sint Annaland, M., and Romano, M. C. (2019b). Techno-economic analysis of a natural gas combined cycle integrated with a Ca-Cu looping process for low CO2 emission power production. *Int. J. Greenh. Gas. Con.* 81, 216–239. doi: 10.1016/j.ijggc.2018.12.026

Martini, M., Martinez, I., Romano, M. C., Chiesa, P., Gallucci, F., and van Sint Annaland, M. (2017). Increasing the carbon capture efficiency of the Ca/Cu looping process for power production with advanced process schemes. *Chem. Eng. J.* 328, 304–319. doi: 10.1016/j.cej.2017.07.048

Martini, M., van den Berg, A., Gallucci, F., and van Sint Annaland, M. (2016). Investigation of the process operability windows for Ca-Cu looping for hydrogen production with CO2 capture. *Chem. Eng. J.* 303, 73–88. doi: 10.1016/j.cej.2016.05.135

Nishioka, K., Ujisawa, Y., Tonomura, S., Ishiwata, N., and Sikstrom, P. (2016). Sustainable aspects of CO2 ultimate reduction in the steelmaking process

(COURSE50 Project), part 1: hydrogen reduction in the blast furnace. *J. Sustain Metall.* 2, 200–208. doi: 10.1007/s40831-016-0061-9

Noorman, S., Gallucci, F., van Sint Annaland, M., and Kuipers, H. (2010). Experimental investigation of a CuO/Al2O3 oxygen carrier for chemical-looping combustion. *Ind. Eng. Chem. Res.* 49, 9720–9728.

Noorman, S., van Sint Annaland, M., and Kuipers, H. (2007). Packed bed reactor technology for chemical-looping combustion. *Ind. Eng. Chem. Res.* 46, 4212–4220. doi: 10.1021/ie061178i

Riva, L., Martínez, I., Martini, M., Gallucci, F., van Sint Annaland, M., and Romano, M. C. (2018). Techno-economic analysis of the Ca-Cu process integrated in hydrogen plants with CO2 capture. *Int. J. Hydrogen Energ.* 43, 15720–15738. doi: 10.1016/j.ijhydene.2018.07.002

Sakaria, D. (2017). "Case Study: Al Reyadah CCUS Project," in *Carbon Sequestration Leadership Forum*, (United Arab Emirates: Abu Dhabi Carbon Capture Company - Al Reyadah).

Santos, S. (2013). *Overview of the Current State and Development of CO2 Capture Technologies In the Ironmaking Process.* Cheltenham: IEA Publications.

Spallina, V., Marinello, B., Gallucci, F., Romano, M. C., and van Sint Annaland, M. (2017). Chemical looping reforming in packed-bed reactors: Modelling, experimental validation and large-scale reactor design. *Fuel Proces. Technol.* 156, 156–170. doi: 10.1016/j.fuproc.2016.10.014

Spallina, V., Romano, M. C., Chiesa, P., Gallucci, F., van Sint Annaland, M., and Lozza, G. (2014). Integration of coal gasification and packed bed CLC for high efficiency and near-zero emission power generation. *Int. J. Greenh. Ga.s Con.* 27, 28–41. doi: 10.1016/j.ijggc.2014.04.029

Tian, S., Li, K., Jiang, J., Chen, X., and Yan, F. (2016). CO2 abatement from the iron and steel industry using a combined Ca-Fe chemical loop. *Appl. Energ.* 170, 345–352. doi: 10.1016/j.apenergy.2016.02.120

Tonomura, S. (2013). Outline of Course 50. *Energy Procedia* 37, 7160–7167. doi: 10.1016/j.egypro.2013.06.653

Tsupari, E., Karki, J., Arasto, A., and Pisila, E. (2013). Post-combustion capture of CO2 at an integrated steel mill – part II: economic feasibility. *Int. J. Greenh. Gas. Con.* 16, 278–286. doi: 10.1016/j.ijggc.2012.08.017

Valverde, J. M. (2013). Ca-based synthetic materials with enhanced CO2 capture efficiency. *J. Mater. Chem. A* 1, 447–468. doi: 10.1039/c2ta00096b

van der Stel, J., Louwerse, G., Sert, D., Hirch, A., Eklund, N., and Pettersson, M. (2013). Top gas recycling blast furnace developments for 'green' and sustainable steelmaking. *Ironmak. Steelmak.* 40, 483–489. doi: 10.1179/0301923313z.000000000221

van Selow, E. R., Cobden, P. D., Verbraeken, P. A., Hufton, J. R., and van den Brink, R. W. (2009). Carbon capture by sorption-enhanced Water-Gas shift reaction process using hydrotalcite-based material. *Ind. Eng. Chem. Res.* 48, 4184–4193. doi: 10.1021/ie801713a

ZEP (2015). *CCS for Industry: Modelling the Lowest-Cost Route for Decarbonizing Europe.* Atlanta, GA: ZEP.